TECHNICAL NOTES   **Open Access**

CrossMark

Measuring inorganic phosphate and intracellular pH in the healthy and hypertrophic cardiomyopathy hearts by in vivo 7T ^{31}P-cardiovascular magnetic resonance spectroscopy

Ladislav Valkovič[1,2]*, William T. Clarke[1,3], Albrecht I. Schmid[1,4], Betty Raman[1], Jane Ellis[1], Hugh Watkins[1], Matthew D. Robson[1], Stefan Neubauer[1] and Christopher T. Rodgers[1,5]

Abstract

Background: Cardiovascular phosphorus MR spectroscopy (^{31}P-CMRS) is a powerful tool for probing energetics in the human heart, through quantification of phosphocreatine (PCr) to adenosine triphosphate (ATP) ratio. In principle, ^{31}P-CMRS can also measure cardiac intracellular pH (pH_i) and the free energy of ATP hydrolysis (ΔG_{ATP}). However, these require determination of the inorganic phosphate (Pi) signal frequency and amplitude that are currently not robustly accessible because blood signals often obscure the Pi resonance.

Typical cardiac ^{31}P-CMRS protocols use low (e.g. 30°) flip-angles and short repetition time (TR) to maximise signal-to-noise ratio (SNR) within hardware limits. Unfortunately, this causes saturation of Pi with negligible saturation of the flowing blood pool. We aimed to show that an adiabatic 90° excitation, long-TR, 7T ^{31}P-CMRS protocol will reverse this balance, allowing robust cardiac pH_i measurements in healthy subjects and patients with hypertrophic cardiomyopathy (HCM).

Methods: The cardiac Pi T_1 was first measured by the dual TR technique in seven healthy subjects. Next, ten healthy subjects and three HCM patients were scanned with 7T ^{31}P-MRS using long (6 s) TR protocol and adiabatic excitation. Spectra were fitted for cardiac metabolites including Pi.

Results: The measured Pi T_1 was 5.0 ± 0.3 s in myocardium and 6.4 ± 0.6 s in skeletal muscle. Myocardial pH was 7.12 ± 0.04 and Pi/PCr ratio was 0.11 ± 0.02. The coefficients of repeatability were 0.052 for pH and 0.027 for Pi/PCr quantification. The pH in HCM patients did not differ ($p = 0.508$) from volunteers. However, Pi/PCr was higher (0.24 ± 0.09 vs. 0.11 ± 0.02; $p = 0.001$); Pi/ATP was higher (0.44 ± 0.14 vs. 0.24 ± 0.05; $p = 0.002$); and PCr/ATP was lower (1.78 ± 0.07 vs. 2.10 ± 0.20; $p = 0.020$), in HCM patients, which is in agreement with previous reports.

(Continued on next page)

* Correspondence: ladislav.valkovic@cardiov.ox.ac.uk
[1]Oxford Centre for Clinical Magnetic Resonance Research (OCMR), Division of Cardiovascular Medicine, BHF Centre of Research Excellence, University of Oxford, Oxford, UK
[2]Department of Imaging Methods, Institute of Measurement Science, Slovak Academy of Sciences, Bratislava, Slovakia
Full list of author information is available at the end of the article

(Continued from previous page)

Conclusion: A 7T ^{31}P-CMRS protocol with adiabatic 90° excitation and long (6 s) TR gives sufficient SNR for Pi and low enough blood signal to permit robust quantification of cardiac Pi and hence pH$_i$. Pi was detectable in every subject scanned for this study, both in healthy subjects and HCM patients. Cardiac pH$_i$ was unchanged in HCM patients, but both Pi/PCr and Pi/ATP increased that indicate an energetic impairment in HCM. This work provides a robust technique to quantify cardiac Pi and pH$_i$.

Keywords: ^{31}P CMRS, 7T, Cardiac intracellular pH, 3D-CSI, Cardiac Pi

Background

Phosphorus cardiovascular magnetic resonance spectroscopy (^{31}P-CMRS) is a valuable technique for non-invasive measurement of high-energy metabolites, e.g. adenosine triphosphate (ATP) and phosphocreatine (PCr), that allows assessment of tissue energy metabolism in vivo [1, 2]. The cardiac PCr/ATP ratio has been established as a biomarker that changes in most major cardiac disease states [3–5], and which predicts mortality in patients with dilated cardiomyopathy [3]. Decreased cardiac PCr/ATP ratios are also observed in obesity [6] and type-II diabetes [7], revealing cardiac involvement in these systemic diseases.

In principle, ^{31}P-CMRS can also be used to measure cardiac intracellular pH (pH$_i$) and the free energy change of ATP hydrolysis (ΔG_{ATP}). However, these require accurate determination of the inorganic phosphate (Pi) signal frequency and amplitude. These are currently not robustly accessible because signals from 2,3-diphosphoglycerate (2,3-DPG) in the ventricular blood pools often obscure the signal from Pi in the myocardium.

Several groups reported pH$_i$ and the Pi/PCr ratio measured in patients with hypertrophic cardiomyopathy (HCM) by ^{1}H-decoupled ^{31}P-CMRS at 1.5 T in the 1990s [8, 9]. In healthy subjects, the detection of cardiac Pi using ^{1}H-decoupling was not possible in all subjects, primarily due to the small concentration of Pi in the heart and the inherently low signal-to-noise ratio (SNR) of ^{31}P-CMRS at 1.5T [9]. Scanning at ultra-high field (7T) increases the SNR of cardiac ^{31}P-CMRS substantially [10]. Additionally, it also enhances the spectral separation between signals from different metabolites. This may enable detection of cardiac Pi without ^{1}H-decoupling, which is infeasible at 7T due to limits on specific absorption rate (SAR). However, typical ^{31}P cardiac spectra are acquired using short TR of about 1 s, and low flip-angle to maximize the SNR/time [10]. Based on skeletal muscle data [11], it can be expected that cardiac Pi will have relatively long relaxation time T$_1$ (several seconds), and thus, experience strong partial saturation. At the same time, the majority of blood in the ventricles is replenished at each heartbeat, so the undesired 2,3-DPG signal is undiminished when scanning with a surface radiofrequency (RF) coil, as is the case in almost all cardiac ^{31}P-CMRS studies [12].

Furthermore, it is essential to know the excitation flip-angle for quantification of metabolite ratios, e.g., Pi/PCr. Regrettably, surface RF coils have a transmit field (B$_1^+$) that drops off rapidly with distance from the coil. This makes metabolite quantification difficult, especially at ultra-high fields. We recently demonstrated feasibility of excitation with a B$_1^+$-insensitive 90° adiabatic pulse for cardiac ^{31}P-CMRS at 7T, which simplifies the quantification of metabolite ratios [13].

The aim of this work was to test the performance and robustness of a cardiac 7T ^{31}P-CMRS protocol with a relatively long TR = 6 s and 90° adiabatic excitation for quantification of cardiac intracellular pH (pH$_i$) and Pi/PCr ratio in the human heart. To this end, we also measured the T$_1$ relaxation time of cardiac Pi using the dual TR technique [14] in seven healthy subjects; performed test-retest reproducibility of intracellular pH calculation in eight healthy subjects; and demonstrated our approach in three patients with HCM.

Methods

All measurements were performed on a 7T whole body, research-only MR system (Siemens Healthineers, Erlangen, Germany) equipped with a custom-built dual-tuned (^{31}P/^{1}H) surface RF-coil, comprising a quadrature ^{31}P coil (two 15 cm loops, with overlap decoupling) and a single ^{1}H loop (10 cm in diameter) for localization (Fig. 1) [15]. The coil was positioned over the heart of participants lying supine. No cardiac gating or respiratory triggering were used [10].

In vivo experiments

In total, 12 healthy subjects (27 ± 5 years; 3 females) and three HCM patients were recruited in compliance with local regulations and institutional ethics committee after giving informed consent. The in vivo experiments can be divided into three main groups: (a) direct comparison of short TR and long TR acquisition, using an amplitude modulated excitation pulse, or a B$_1^+$ insensitive adiabatic half-passage (AHP) pulse; (b) measurement of T$_1$ of cardiac Pi; and (c) quantification of cardiac Pi/PCr and pH$_i$ in healthy subjects and HCM patients. Some of the subjects took part in several of the in vivo experiments.

The feasibility to detect cardiac Pi using long vs short TR was first tested in one healthy subject by using two
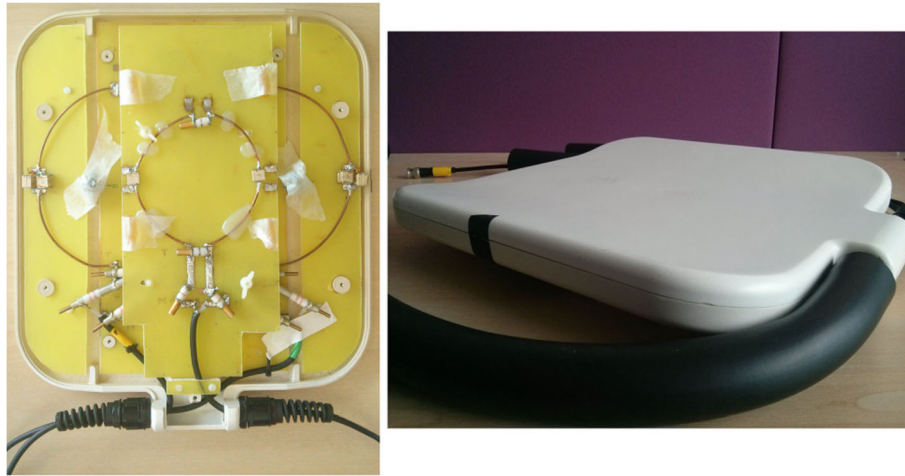
Fig. 1 A photograph of our custom-built dual-tuned (^{31}P/^{1}H) surface RF-coil, comprising a quadrature ^{31}P coil (two 15 cm loops, with overlap decoupling) and a single ^{1}H loop (10 cm in diameter) described in detail in Schaller et al. [15]

consecutive 3D ultrashort echo time (UTE) chemical shift imaging (CSI) [16] acquisitions. The first had a "short" (1 s) TR, and the other a "long" (5 s) TR. Both had matrix size ($8 \times 16 \times 8$), field of view (FOV) ($240 \times 240 \times 200$ mm^3) and used acquisition weighting. This translates into an effective voxel size of 50.7mL [13]. The number of averages (NA) was matched for equal acquisition time, giving 41 averages for the short and 5 averages for the long TR measurement. An amplitude-modulated excitation pulse (1 ms long) applied in previous 7T studies was used [10].

Next, the recently proposed AHP pulse [13] was applied in three volunteers. In order to use this relatively SAR demanding pulse (7.5 ms long) with short TR (1 s), the 3D UTE-CSI [16] sequence was modified to allow an interleaved TR acquisition with two different TRs [17]. In this case, the second TR was matched to the effective TR in the AHP study, i.e. 6 s TR [13]. Matrix size and FOV matched the first experiment and acquisition weighting with 5 averages at the centre of k space was used for both TRs. The excitation frequency of the AHP pulse was centred at the 2,3-DPG signal, i.e. + 700 Hz relative to PCr.

Seven subjects were consecutively scanned using the dual TR technique [14] for determination of the T_1 of cardiac Pi, which is required for quantification of the detected myocardial Pi. Since the interleaved TR acquisition is not suitable for T_1 determination [17], two successive 3D UTE-CSI [16] acquisitions were required. The SAR limits for the narrow-banded AHP pulse [13] we used allowed for a 3 s minimum TR. Our chosen TR values were therefore: $TR_1 = 3$ s and $TR_2 = 6$ s. The matrix size and FOV again matched the original protocol, i.e. $8 \times 16 \times 8$ and $240 \times 240 \times 200$ mm^3, respectively. The AHP pulse we used has a relatively narrow
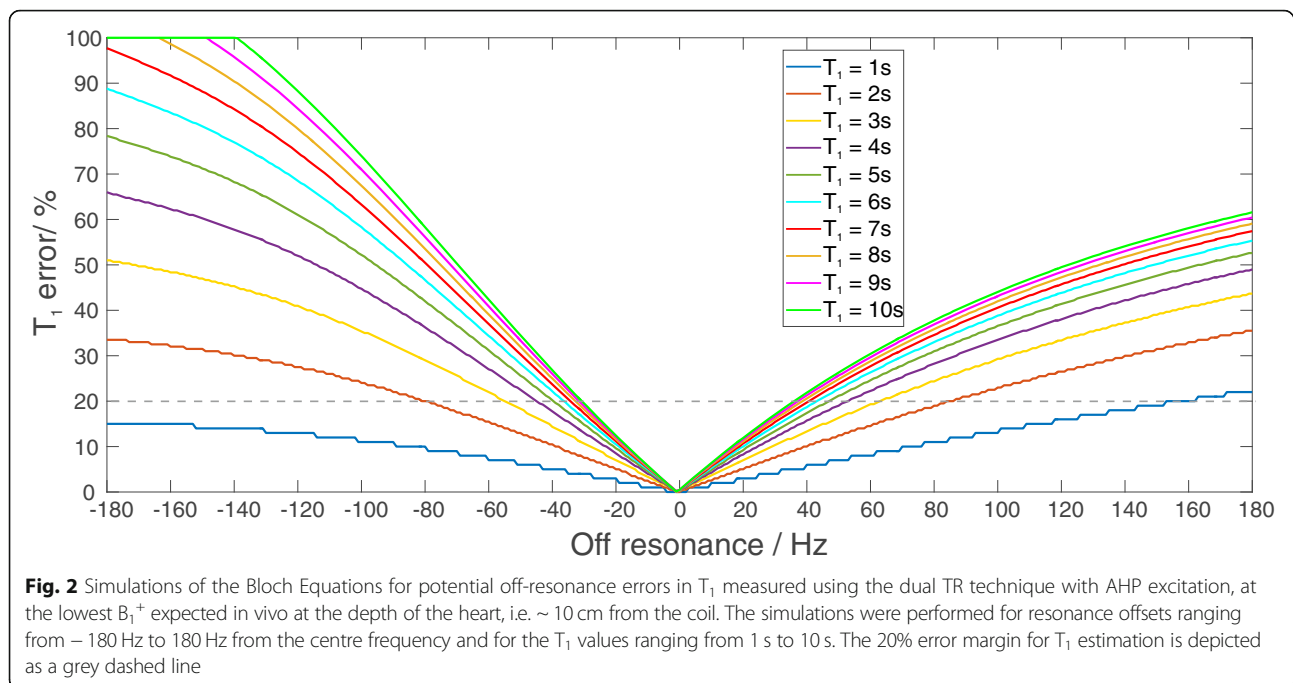
bandwidth for typical B_1^+ in the heart for our coil. So, the excitation was centred at + 600 Hz from PCr and the smooth side of the pulse's frequency profile was facing towards PCr. Numerical solutions of the Bloch Equations were performed in Matlab (MathWorks, Natick, Massachusetts, USA) to estimate the potential errors in calculated T_1 for resonance offsets from − 180 Hz to + 180 Hz from centre frequency, for the T_1 values from 1 s to 10 s (Fig. 2).

Ten healthy subjects then underwent cardiac 7T ^{31}P-CMRS examinations for cardiac pH, Pi/PCr and Pi/ATP quantification using interleaved AHP excitation [13]. In short, the AHP excitation was interleaved to excite the PCr and ATP region in odd acquisitions and the Pi and DPG region in even acquisitions. The effective TR was 6 s and other parameters matched the T_1 measurements. The total acquisition time was 46 min and 42 s. In a subset of these subjects ($n = 8$), the measurement was performed twice to assess the repeatability of cardiac pH$_i$ and Pi/PCr determination.

Finally, to demonstrate the feasibility of the technique in patients, three male patients with established diagnoses of HCM (57 ± 12 years, mean wall thickness 21 ± 2 mm) were recruited and scanned with the interleaved AHP protocol [13] to determine their cardiac pH, Pi/PCr and Pi/ATP. The acquisition time for patients was the same as for healthy subjects, i.e. 46 min and 42 s.

Data analysis
For each subject, three septal voxels in the two mid left ventricular slices (six in total) were selected for further analysis. In addition, six chest muscle voxels were also selected for the T_1 analysis. Spectra from all selected voxels were fitted using the OXSA toolbox [18] and its implementation of the AMARES time-domain fitting

Fig. 2 Simulations of the Bloch Equations for potential off-resonance errors in T_1 measured using the dual TR technique with AHP excitation, at the lowest B_1^+ expected in vivo at the depth of the heart, i.e. ~ 10 cm from the coil. The simulations were performed for resonance offsets ranging from − 180 Hz to 180 Hz from the centre frequency and for the T_1 values ranging from 1 s to 10 s. The 20% error margin for T_1 estimation is depicted as a grey dashed line

algorithm [19]. The PCr signal, fitted as single Lorentzian, and the γ-ATP signal, fitted as a Lorentzian doublet, were quantified from the odd acquisition spectra. The Pi and 2,3-DPG signals, all fitted as single Lorentzians, were quantified from the even acquisition spectra. The resonance frequency of Pi was constrained to the 4.7–5.1 ppm range and the two 2,3-DPG peaks were constrained to 5.2–5.7 ppm and 6.0–6.3 ppm, respectively. The same constraints for linewidth, i.e. 20-60 Hz, without dependencies on other peaks were applied for both 2,3-DPG signals and for Pi signal. If a limit was reached during fitting, fitting was repeated with the constraints extended by ±5 Hz.

The T_1 relaxation of Pi was determined in cardiac and skeletal muscle voxels using the dual TR technique [14]. ATP and Pi signals were corrected for blood contamination as previously described [20]. Cramér-Rao lower bounds (CRLB) [21] were determined for the Pi peak amplitudes and voxels with the CRLB ≥15% were excluded. Remaining cardiac data were further corrected for partial saturation effects using the calculated T_1 values for Pi and literature T_1 values for γ-ATP and PCr [10]. As our voxels are relatively big, to confirm that the quantification of Pi did not depend on how much blood contamination was in the voxel, we have performed a correlation analysis between our reported blood-corrected Pi/PCr values and the 2,3-DPG/PCr ratio using all evaluated voxels, i.e. including the repeatability data. The cardiac intracellular pH_i was calculated from the chemical shift between Pi and PCr using the modified Henderson-Haselbach equation [22]. The Pi/PCr ratio and pH_i were compared between the two repeated

measurements of healthy subjects by Bland-Altman analysis of agreement [23]. Coefficients of repeatability were estimated as $1.96 \times \sqrt{2} \times$ intra-subject standard deviation (SD) [24]. Data are presented as mean ± SD. Student's t-test was used to compare the PCr/ATP, Pi/ATP, Pi/PCr and pH_i of healthy subjects and HCM patients, with $p < 0.05$ considered statistically significant.

Results

In the datasets acquired using the short TR, it was not possible to distinguish a Pi peak in voxels of interventricular septum, due to strong overlapping 2,3-DPG signals from blood. Although similarly strong 2,3-DPG signals were observed in the data acquired with long TR, the long TR acquisition allowed clear visibility of the Pi peak above 2,3-DPG in these voxels (Fig. 3).

Our Bloch simulations showed that the error in T_1 estimation, using the dual TR technique and selected TRs of 3 s and 6 s, increases with increasing frequency offset (Fig. 2). There is a steeper rise in T_1 error on the sharper side of the AHP pulse frequency profile. Nevertheless, T_1 errors < 20% are predicted for frequency offsets between − 30 Hz and + 35 Hz throughout the simulated T_1 range (1–10 s). Representative spectra from skeletal muscle and interventricular septum are depicted in Fig. 4. The mean measured T_1 relaxation time of Pi was 6.4 ± 0.6 s in chest muscle tissue and 5.0 ± 0.3 s in interventricular septum.

In total, 108 septal voxels were analysed for pH and Pi quantification in healthy subjects, i.e. 6 voxels per measurement ($n = 18$, including the scan-rescan data). Out of
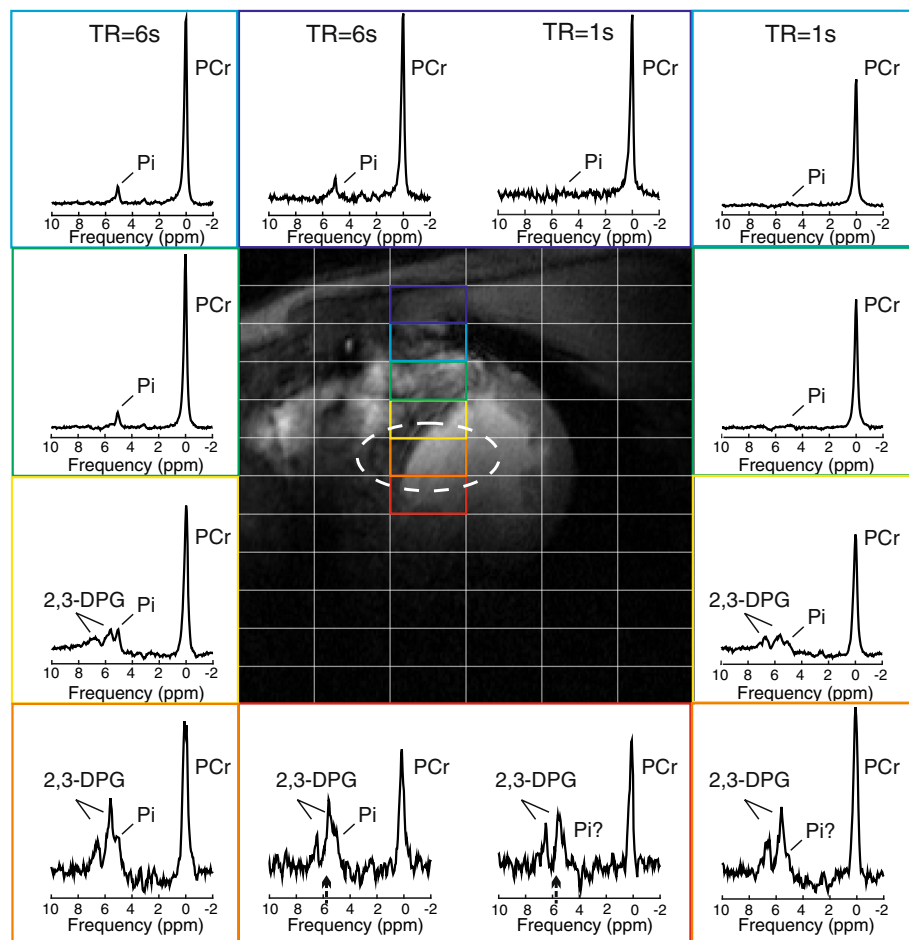
Fig. 3 Spectra acquired with the interleaved TR sequence using a single AHP excitation frequency centred at the 2,3-DPG resonance (marked with a black arrow near the x-axis in the red voxel spectra). Spectra are shown for voxels in the chest wall muscle down to the intraventricular septum. Note the increased Pi amplitude in all voxels acquired at longer TR, demonstrating the improved detectability of Pi, which allows for reliable cardiac pH$_i$ determination. The effective voxel size is depicted using a dashed white line

these, 93 voxels had CRLB of Pi < 15%, with the mean CRLB of $10.6 \pm 1.8\%$. On average, 5.2 ± 1.0 voxels per dataset were analysed further, with at least 4 voxels used in 17 datasets and 2 voxels in one. Figure 5 depicts a representative fit of a cardiac voxel acquired during the even acquisition.

Table 1 denotes the calculated metabolite ratios and cardiac pH$_i$ for each subject. The mean myocardial pH of healthy subjects was 7.12 ± 0.04 and the Pi/PCr ratio was 0.11 ± 0.02. Figure 6 depicts the Bland-Altman plots of the in vivo test-retest measurements of myocardial pH and Pi/PCr. The mean absolute biases given by the analysis of agreement were only 0.007 and 0.003, with the limits of agreement of ± 0.069 and ± 0.036 for pH and Pi/PCr, respectively. The estimated repeatability coefficients were 0.052 and 0.027 for pH and Pi/PCr, respectively. No correlation was found between the blood-corrected Pi/PCr and 2,3-DPG/PCr values in this study ($r = 0.001$, $p = 0.992$).

Figure 7 shows representative septal spectra acquired in a healthy subject and an HCM patient. More dominant cardiac Pi signal can be seen in the patient's spectrum. A lower PCr/ATP ratio (1.78 ± 0.07 vs. 2.10 ± 0.20; $p = 0.020$) and higher Pi/ATP (0.44 ± 0.14 vs. 0.24 ± 0.05; $p = 0.002$) and Pi/PCr (0.24 ± 0.09 vs. 0.11 ± 0.02; $p = 0.001$) ratios were found in HCM patients compared to young healthy subjects. Detailed information is given in Table 1.

Discussion

We proposed using 7T ^{31}P-CMRS with adiabatic excitation and long TRs to quantify cardiac Pi and determine pH$_i$ in vivo. Our results show that this approach allows robust detection of cardiac Pi in healthy subjects and also patients with HCM. The direct detection of cardiac Pi makes cardiac pH$_i$ determination straightforward. We demonstrated excellent repeatability of this method, with limits of agreement: ± 0.069 and ± 0.036 for pH and Pi/
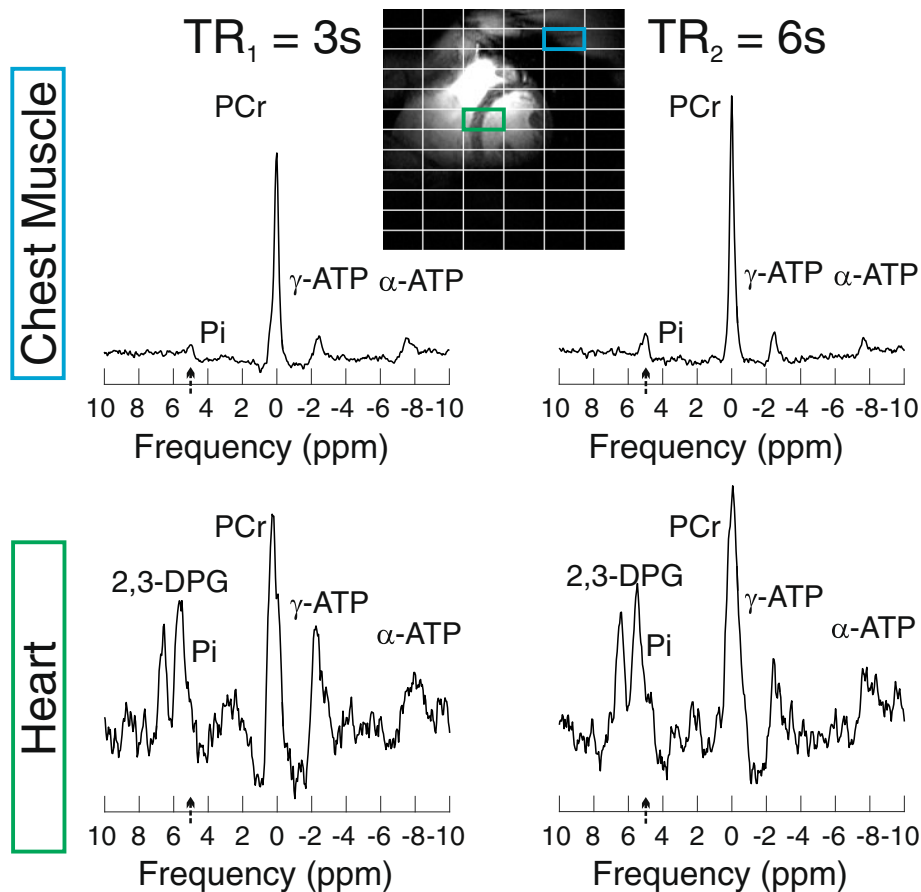
Fig. 4 ^{31}P-CMRS spectra acquired in the chest muscle (blue voxel - upper row) and human heart (green voxel - bottom row) with $TR_1 = 3$ s (left) and $TR_2 = 6$ s (right). Spectra were acquired with a single AHP excitation frequency centred on Pi (marked with a black arrow near the x-axis). Please note that while spectra are scaled equally for TR_1 and TR_2, the heart spectra are scaled differently than the skeletal muscle spectra. A 30 Hz Lorentzian filter was applied to all spectra for better visualization. A pronounced Pi signal can be seen in TR_2 spectra both in chest muscle and in the heart. Due to the limited excitation bandwidth of the AHP pulse, β-ATP peak is not excited, and thus, not shown

PCr, respectively. We also measured the T_1 for myocardial Pi at 7T, which permits quantification of cardiac Pi/PCr.

Our protocol using long TR acquisition and adiabatic 90° excitation at 7T allowed for detection of myocardial Pi in vivo. In typical cardiac ^{31}P-CMRS experiments, Pi is obscured by a dominant overlapping signal from 2,3-DPG in the blood pool. This approach is successful because the long TR reduces the effect of partial T_1 saturation on Pi, which in typical short TR acquisitions strongly reduces the myocardial tissue signal leaving the 2,3-DPG signal from in-flowing blood almost intact. We demonstrated the effect of TR on Pi detection by comparing long and short TR acquisitions in the same subjects.

The majority of previously published studies quantifying cardiac pH$_i$ by ^{31}P-CMRS used ^{1}H-decoupling to reduce the 2,3-DPG linewidth and minimise overlap with Pi [8, 9]. Although, ^{1}H-decoupled 1.5 T ^{31}P-CMRS was shown to be effective in HCM patients, its feasibility in

healthy subjects was limited, e.g. de Roos et al. reported a 44% success rate ($n = 4/9$) in healthy subjects [9]. Jung et al. were able to reliably fit myocardial Pi in only 82% ($n = 9/11$) of cases [8]. In 100% of our healthy subject ($n = 18/18$), it was possible to find at least two septal voxels where AMARES fitted the Pi peak reliably (i.e. with CRLB < 15%), and in 94% cases we were able to fit Pi robustly in at least four out of our six targeted voxels. The improved SNR from scanning at 7T makes our approach robust. In future, we envisage that optimised per-subject B_0 shimming would further aid separation of Pi and 2,3-DPG signals in our approach [25]. An alternative technique for determining cardiac pH$_i$ was introduced by Blamire et al., who recorded spectra with and without saturation of the γ-ATP resonance. Subtracting these spectra suppresses 2,3-DPG and leaves signal from Pi generated by ATP hydrolysis [26]. They also achieved a 100% success rate ($n = 6/6$) for cardiac pH$_i$ determination but unlike our method, their approach does not allow
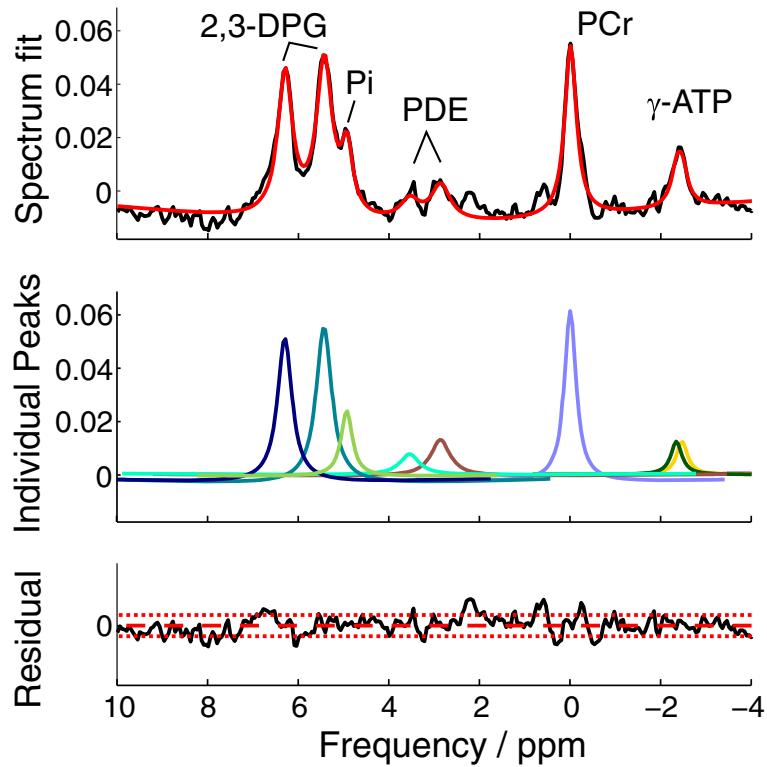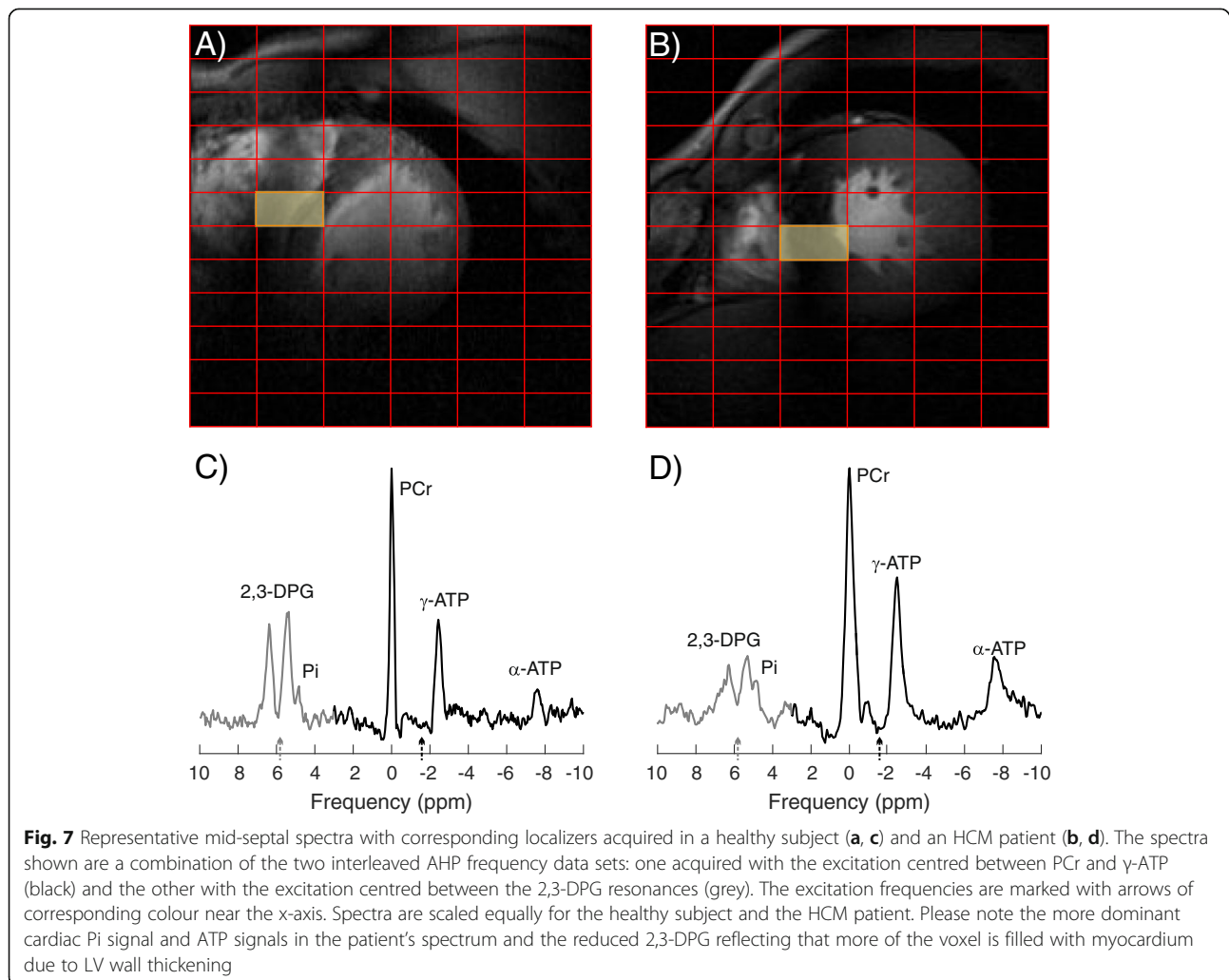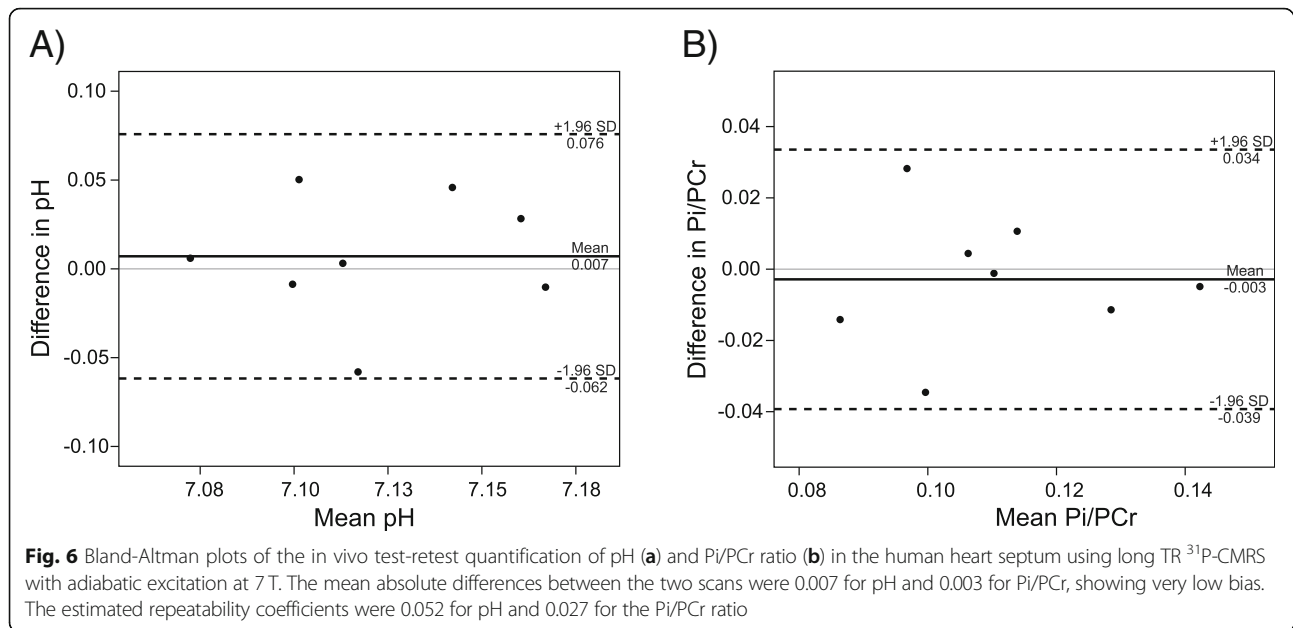
Fig. 5 A representative result of the fitting procedure. A mid-septal spectrum measured during an even acquisition overlaid by the final spectral fit (top); individual peaks fitting (middle) and the residual (bottom) is depicted

Table 1 Calculated metabolite ratios and cardiac pH_i for every volunteer and patient

Participant	PCr/ATP		Pi/ATP		Pi/PCr		pH	
	Meas.1	Meas.2	Meas.1	Meas.2	Meas.1	Meas.2	Meas.1	Meas.2
Healthy subject #1	1.79 ± 0.39	1.86 ± 0.51	0.22 ± 0.19	0.24 ± 0.17	0.12 ± 0.10	0.13 ± 0.09	7.10 ± 0.13	7.10 ± 0.06
Healthy subject #2	2.15 ± 0.68	2.28 ± 1.09	0.25 ± 0.14	0.17 ± 0.10	0.11 ± 0.03	0.08 ± 0.04	7.08 ± 0.15	7.07 ± 0.07
Healthy subject #3	1.82 ± 0.38	2.04 ± 0.44	0.24 ± 0.08	0.29 ± 0.09	0.14 ± 0.07	0.14 ± 0.05	7.17 ± 0.28	7.15 ± 0.08
Healthy subject #4	2.25 ± 0.63	2.17 ± 0.63	0.24 ± 0.10	0.22 ± 0.12	0.11 ± 0.04	0.10 ± 0.07	7.16 ± 0.11	7.17 ± 0.04
Healthy subject #5	2.32 ± 0.47	2.37 ± 0.58	0.19 ± 0.10	0.23 ± 0.16	0.08 ± 0.04	0.12 ± 0.11	7.11 ± 0.05	7.11 ± 0.02
Healthy subject #6	2.08 ± 0.41	1.84 ± 0.45	0.17 ± 0.10	0.22 ± 0.05	0.08 ± 0.06	0.09 ± 0.03	7.09 ± 0.05	7.15 ± 0.02
Healthy subject #7	2.14 ± 0.62	2.10 ± 0.68	0.22 ± 0.22	0.23 ± 0.15	0.11 ± 0.12	0.11 ± 0.09	7.13 ± 0.03	7.08 ± 0.02
Healthy subject #8	2.19 ± 0.19	2.37 ± 0.43	0.27 ± 0.12	0.26 ± 0.12	0.12 ± 0.05	0.11 ± 0.05	7.17 ± 0.01	7.12 ± 0.02
Healthy subject #9	2.36 ± 0.53	N/A	0.35 ± 0.24	N/A	0.14 ± 0.10	N/A	7.10 ± 0.05	N/A
Healthy subject #10	1.93 ± 0.57	N/A	0.24 ± 0.11	N/A	0.13 ± 0.06	N/A	7.14 ± 0.06	N/A
Mean	2.10 ± 0.20	2.13 ± 0.21	0.24 ± 0.05	0.23 ± 0.04	0.11 ± 0.02	0.11 ± 0.02	7.12 ± 0.04	7.12 ± 0.04
HCM #1	1.75 ± 0.45		0.48 ± 0.28		0.26 ± 0.12		7.16 ± 0.03	
HCM #2	1.73 ± 0.67		0.56 ± 0.32		0.32 ± 0.16		7.12 ± 0.04	
HCM #3	1.86 ± 0.33		0.28 ± 0.14		0.14 ± 0.05		7.14 ± 0.07	
Mean	1.78 ± 0.07*		0.44 ± 0.14*		0.24 ± 0.09*		7.14 ± 0.02	
% change	−15		+ 83		+ 118		0.21	

Data are given as inter-voxel mean ± SD and the mean data are given as inter-subject mean ± SD, *denotes significant difference ($p < 0.05$) between healthy subjects and HCM patients
Values from both measurements of the repeatability study are given

Fig. 6 Bland-Altman plots of the in vivo test-retest quantification of pH (**a**) and Pi/PCr ratio (**b**) in the human heart septum using long TR ^{31}P-CMRS with adiabatic excitation at 7 T. The mean absolute differences between the two scans were 0.007 for pH and 0.003 for Pi/PCr, showing very low bias. The estimated repeatability coefficients were 0.052 for pH and 0.027 for the Pi/PCr ratio

Fig. 7 Representative mid-septal spectra with corresponding localizers acquired in a healthy subject (**a**, **c**) and an HCM patient (**b**, **d**). The spectra shown are a combination of the two interleaved AHP frequency data sets: one acquired with the excitation centred between PCr and γ-ATP (black) and the other with the excitation centred between the 2,3-DPG resonances (grey). The excitation frequencies are marked with arrows of corresponding colour near the x-axis. Spectra are scaled equally for the healthy subject and the HCM patient. Please note the more dominant cardiac Pi signal and ATP signals in the patient's spectrum and the reduced 2,3-DPG reflecting that more of the voxel is filled with myocardium due to LV wall thickening

for direct Pi/PCr quantification because Pi is visible only in the difference spectrum [26].

We have measured the T_1 of Pi in myocardial septum as well as in skeletal muscle, to allow quantification of Pi. This was possible using the dual TR technique [14]. Although the shortest possible TR was limited by SAR, our simulations show that our TRs would have < 20% error in T_1. The method can tolerate 0.5 ppm mis-adjustment of the ^{31}P transmitter frequency. The mean T_1 value we measured in the chest muscle (6.4 ± 0.6 s) is in good agreement with literature [10, 11]. Our mean measured T_1 value for cardiac Pi (5.0 ± 0.3 s) was shorter than the literature values measured in the calf muscle at 7T (6.3 ± 1.0 s [11] and 6.7 ± 0.2 s [10]). This is in agreement with shorter T_1 times of PCr and ATP reported in the heart in comparison to skeletal muscle [10]. Our T_1 of Pi measured in human heart is also in good accordance with the value reported for 2 T (4.3 ± 2.4 s) [27] given that T_1 values change with field strength [11].

We found no significant difference in cardiac pH_i between healthy subjects and HCM patients (7.12 ± 0.04 vs 7.14 ± 0.02; $p = 0.508$). Even though our patient sample is rather small, this agrees with previous reports [8, 9, 28]. Our measured cardiac pH_i agrees with literature values showing mean cardiac pH_i ranging from 7.06 to 7.15 for healthy subjects [8, 9, 26, 28, 29]. Furthermore, our repeatability test showed good agreement between the cardiac pH_i measured in the two acquisitions, with the limits of agreement being 0.007 ± 0.069 and the estimated repeatability coefficient being 0.052. This is to our knowledge the first published reproducibility for cardiac pH_i measurement published.

Previous studies have reported both a reduced PCr/ATP and an increased Pi/PCr in HCM patients compared to healthy subjects [8, 9, 28, 30]. In line with these findings, we have found a lower PCr/ATP ratio in HCM patients (1.78 ± 0.07 vs. 2.10 ± 0.20; − 15%; $p = 0.020$). Furthermore, Pi/PCr (0.24 ± 0.09 vs. 0.11 ± 0.02; 118%; $p = 0.001$) and Pi/ATP (0.44 ± 0.14 vs. 0.24 ± 0.05; 83%; $p = 0.002$) ratios were significantly higher in HCM compared to controls. Comparing absolute numbers, de Roos et al. [9] reported Pi/PCr ratios of 0.14 ± 0.06 and 0.20 ± 0.04 for healthy subjects and HCM patients, i.e. a 43% increase. Similarly, Jung et al. [8] reported 0.10 ± 0.07 and 0.20 ± 0.08 Pi/PCr ratios in healthy control subjects and HCM patients, i.e. an increase of 100%. We observed a slightly larger (118%) increase of Pi/PCr ratios in HCM patients, albeit in a small cohort. Our Bland-Altman analysis of agreement between repeated measurements of Pi/PCr ratio showed limits of agreement of − 0.003 ± 0.036 and the estimated repeatability coefficient was 0.027. It has been proposed previously that increased Pi in the

heart may directly inhibit contractile function since the release of Pi from the actin-myosin cross bridge is associated with force development [31] and was shown to correlate with the myocardial contractile force at the onset of ischemia in animal studies [32]. It has been also suggested lately that the Pi is both the primary feedback signal for stimulating oxidative phosphorylation in vivo and also the most significant product of ATP hydrolysis in limiting the capacity of the heart to hydrolyse ATP in vivo [33]. The scope of this technical work was limited, and thus at this time we can neither confirm nor refute these previous findings on the changes in Pi and pH_i due to HCM. However, this work paves the way for studies that will be able to test these theories in more adequately powered larger patient cohorts.

The main limitation of our study is the relatively long acquisition time required (47 min) due to the combination of 3D-CSI localisation and long 6 s TR. However, trying to shorten the scan time by reducing the TR would limit the detectability of cardiac Pi, and it would also likely exceed SAR restrictions because of the adiabatic excitation pulses used [13]. Faster localization strategies, e.g., 1D-image selected in vivo spectroscopy (1D-ISIS) or 1D-CSI could potentially be combined with our approach for cardiac Pi detection, but our RF-coil has insufficient peak B_1^+ for an effective inversion pulse and too large a sensitive volume for effective localisation of cardiac signal by 1D-ISIS or 1D-CSI [13]. Acquisition of data with higher spatial resolution, i.e. smaller voxel size, could also help to minimize the signal contamination from the blood pool, but this again requires comparably long acquisition time even with a short TR and reduced number of averages, which could in turn limit the detectability of cardiac Pi in healthy subjects [34].

Conclusion

In conclusion, we present a technique for reliable quantitation of cardiac Pi and determination of cardiac intracellular pH (pH_i) using 7T ^{31}P-CMRS with adiabatic excitation and a long TR. We achieved 100% success rate for Pi detection in the hearts of 10 consecutively recruited healthy subjects and in three HCM patients. We were also able to measure the longitudinal relaxation time of cardiac Pi at 7T. This allowed for quantification of the cardiac Pi/PCr and Pi/ATP ratios, which were significantly increased in three patients with HCM. This new technique will allow addressing an array of clinically relevant questions related to the role of Pi in cardiac diseases.

HCM: Hypertrophic cardiomyopathy; NA: Number of averages; PCr: Phosphocreatine; Pi: Inorganic phosphate; RF: Radiofrequency; SAR: Specific absorption rate; SD: Standard deviation; SNR: Signal-to-noise ratio; TR: Repetition time; UTE-CSI: Ultrashort echo time chemical shift imaging

Availability of data and materials
The datasets generated and/or analysed during the current study are available from the corresponding author on reasonable request.

Authors' contributions
LV: participated in all aspects of the study and drafted the manuscript. WTC: made substantial contributions to conception and design of the study and revised the manuscript critically for important intellectual content. AIS: made substantial contributions to analysis and interpretation of data and revised the manuscript critically for important intellectual content. BR: made substantial contributions to acquisition of data. JE: made substantial contributions to acquisition of data. HW: made substantial contributions to acquisition of data and revised the manuscript critically for important intellectual content. MDR: made substantial contributions to conception and design of the study. SN: made substantial contributions to conception and design of the study and revised the manuscript critically for important intellectual content. CTR: participated in all aspects of the study and revised the manuscript critically for important intellectual content. All authors read and approved the final version of the manuscript.

Ethics approval and consent to participate
The study was approved by the institutional ethics committee (reference12/LO/1979).

Consent for publication
Consent for publication of details and accompanying images of the recruited subjects was provided. No protected health information for any subject is given in this manuscript.

Competing interests
The authors declare that they have no competing interests.

Publisher's Note
Springer Nature remains neutral with regard to jurisdictional claims in published maps and institutional affiliations.

Author details
[1]Oxford Centre for Clinical Magnetic Resonance Research (OCMR), Division of Cardiovascular Medicine, BHF Centre of Research Excellence, University of Oxford, Oxford, UK. [2]Department of Imaging Methods, Institute of Measurement Science, Slovak Academy of Sciences, Bratislava, Slovakia. [3]Wellcome Centre for Integrative Neuroimaging, FMRIB, Nuffield Department of Clinical Neurosciences, University of Oxford, Oxford, UK. [4]High-Field MR Centre, Centre for Medical Physics and Biomedical Engineering, Medical University of Vienna, Vienna, Austria. [5]The Wolfson Brain Imaging Centre, University of Cambridge, Cambridge Biomedical Campus, Cambridge, UK.

References
1. Bottomley PA, Charles HC, Roemer PB, Flamig D, Engeseth H, Edelstein WA, Mueller OM. Human in vivo phosphate metabolite imaging with 31P NMR. Magn Reson Med. 1988;7:319–36.
2. Valkovič L, Chmelík M, Kriššák M. In-vivo 31P-MRS of skeletal muscle and liver: a way for non-invasive assessment of their metabolism. Anal Biochem. 2017;529:193–215.
3. Neubauer S, Horn M, Cramer M, Harre K, Newell JB, Peters W, Pabst T, Ertl G, Hahn D, Ingwall JS, Kochsiek K. Myocardial phosphocreatine-to-ATP ratio is a predictor of mortality in patients with dilated cardiomyopathy. Circulation. 1997;96:2190–6.
4. Bottomley PA. NMR spectroscopy of the human heart. In: Harris RK, Wasylishen RE, editors. Encyclopedia of magnetic resonance. Chichester: John Wiley; 2009.
5. Stoll VM, Clarke WT, Levelt E, Liu A, Myerson SG, Robson MD, Neubauer S. Rodgers CT. Dilated cardiomyopathy: phosphorus 31 MR spectroscopy at 7 T. Radiology. 2016;281:409–17.
6. Rider OJ, Francis JM, Ali MK, Holloway C, Pegg T, Robson MD, Tyler D, Byrne J, Clarke K, Neubauer S. Effects of catecholamine stress on diastolic function and myocardial energetics in obesity. Circulation. 2012;125:1511–9.
7. Levelt E, Rodgers CT, Clarke WT, Mahmod M, Ariga R, Francis JM, Liu A, Wijesurendra RS, Dass S, Sabharwal N, Robson MD, Holloway CJ, Rider OJ, Clarke K, Karamitsos TD, Neubauer S. Cardiac energetics, oxygenation, and perfusion during increased workload in patients with type 2 diabetes mellitus. Eur Heart J. 2016;37:3461–9.
8. Jung WI, Sieverding L, Breuer J, Hoess T, Widmaier S, Schmidt O, Bunse M, van Erckelens F, Apitz J, Lutz O, Dietze GJ. 31P NMR spectroscopy detects metabolic abnormalities in asymptomatic patients with hypertrophic cardiomyopathy. Circulation. 1998;97:2536–42.
9. de Roos A, Doornbos J, Luyten PR, Oosterwaal LJ, van der Wall EE, den Hollander JA. Cardiac metabolism in patients with dilated and hypertrophic cardiomyopathy: assessment with proton-decoupled P-31 MR spectroscopy. J Magn Reson Imaging. 1992;2:711–9.
10. Rodgers CT, Clarke WT, Snyder C, Vaughan JT, Neubauer S, Robson MD. Human cardiac 31P magnetic resonance spectroscopy at 7 tesla. Magn Reson Med. 2014;72:304–15.
11. Bogner W, Chmelik M, Schmid AI, Moser E, Trattnig S, Gruber S. Assessment of 31P relaxation times in the human calf muscle: a comparison between 3 T and 7 T in vivo. Magn Reson Med. 2009;62:574–82.
12. Valkovič L, Dragonu I, Almujayyaz S, Batzakis A, Young LAJ, Purvis LAB, Clarke WT, Wichmann T, Lanz T, Neubauer S, Robson MD, Klomp DWJ, Rodgers CT. Using a whole-body 31P birdcage transmit coil and 16-element receive array for human cardiac metabolic imaging at 7T. PLoS One. 2017;12:e0187153.
13. Valkovič L, Clarke WT, Purvis LAB, Schaller B, Robson MD. Rodgers CT. Adiabatic excitation for 31P MR spectroscopy in the human heart at 7 T: a feasibility study. Magn Reson Med. 2017;78:1667–73.
14. El-Sharkawy AM, Schar M, Ouwerkerk R, Weiss RG. Bottomley PA. Quantitative cardiac 31P spectroscopy at 3 tesla using adiabatic pulses. Magn Reson Med. 2009;61:785–95.
15. Schaller B, Paritmongkol W and Rodgers CT. Quadrature 31P and single 1H dual-tune coil for cardiac 31P-MRS at 7T. In Proceedings of the 24th Annual Meeting of ISMRM, Singapore, Singapore, 2016. p. 4006.
16. Robson MD, Tyler DJ, Neubauer S. Ultrashort TE chemical shift imaging (UTE-CSI). Magn Reson Med. 2005;53:267–74.
17. Yarnykh VL. Actual flip-angle imaging in the pulsed steady state: a method for rapid three-dimensional mapping of the transmitted radiofrequency field. Magn Reson Med. 2007;57:192–200.
18. Purvis LAB, Clarke WT, Biasiolli L, Valkovič L, Robson MD, Rodgers CT. OXSA. An open-source magnetic resonance spectroscopy analysis toolbox in MATLAB. PLoS One. 2017;12:e0185356.
19. Vanhamme L, van den Boogaart A, Van Huffel S. Improved method for accurate and efficient quantification of MRS data with use of prior knowledge. J Magn Reson. 1997;129:35–43.
20. Horn M, Neubauer S, Bomhard M, Kadgien M, Schnackerz K, Ertl G. 31P-NMR spectroscopy of human blood and serum: first results from volunteers and patients with congestive heart failure, diabetes mellitus and hyperlipidaemia. Magma. 1993;1:55–60.

21. Cavassila S, Deval S, Huegen C, van Ormondt D, Graveron-Demilly D. Cramer-Rao bounds: an evaluation tool for quantitation. NMR Biomed. 2001;14:278–83.

22. Moon RB. Richards JH. Determination of intracellular pH by 31P magnetic resonance. J Biol Chem. 1973;248:7276–8.

23. Bland JM, Altman DG. Statistical methods for assessing agreement between two methods of clinical measurement. Lancet. 1986;1:307–10.

24. Bartlett JW, Frost C. Reliability, repeatability and reproducibility: analysis of measurement errors in continuous variables. Ultrasound Obstet Gynecol. 2008;31:466–75.

25. DelaBarre L, Neubauer S, Robson MD, Vaughan JT, Rodgers CT. B0 Shimming Further Improves Human Cardiac 31P-MRS at 7 Tesla. In: Proceedings of the 23rd Annual Meeting of ISMRM. Toronto, Ontario, CA; 2015. p. 3152.

26. Blamire AM, Rajagopalan B, Radda GK. Measurement of myocardial pH by saturation transfer in man. Magn Reson Med. 1999;41:198–203.

27. Bottomley PA, Ouwerkerk R. Optimum flip-angles for exciting NMR with uncertain T1 values. Magn Reson Med. 1994;32:137–41.

28. Sieverding L, Jung WI, Breuer J, Widmaier S, Staubert A, van Erckelens F, Schmidt O, Bunse M, Hoess T, Lutz O, Dietze GJ, Apitz J. Proton-decoupled myocardial 31P NMR spectroscopy reveals decreased PCr/pi in patients with severe hypertrophic cardiomyopathy. Am J Cardiol. 1997;80:34A–40A.

29. Luyten PR, Bruntink G, Sloff FM, Vermeulen JW, van der Heijden JI, den Hollander JA, Heerschap A. Broadband proton decoupling in human 31P NMR spectroscopy. NMR Biomed. 1989;1:177–83.

30. Crilley JG, Boehm EA, Blair E, Rajagopalan B, Blamire AM, Styles P, McKenna WJ, Ostman-Smith I, Clarke K, Watkins H. Hypertrophic cardiomyopathy due to sarcomeric gene mutations is characterized by impaired energy metabolism irrespective of the degree of hypertrophy. J Am Coll Cardiol. 2003; 41:1776–82.

31. Kubler W, Katz AM. Mechanism of early "pump" failure of the ischemic heart: possible role of adenosine triphosphate depletion and inorganic phosphate accumulation. Am J Cardiol. 1977;40:467–71.

32. He MX, Wang S, Downey HF. Correlation between myocardial contractile force and cytosolic inorganic phosphate during early ischemia. Am J Phys. 1997;272:H1333–41.

33. Wu F, Zhang EY, Zhang J, Bache RJ, Beard DA. Phosphate metabolite concentrations and ATP hydrolysis potential in normal and ischaemic hearts. J Physiol. 2008;586:4193–208.

34. Clarke WT. Human Cardiac Magnetic Resonance Spectroscopy, in Oxford Centre for Clinical Magnetic Resonance Research and Worcester College. University of Oxford; 2016.